Examples of Seismic Shallow Subsurface Characterisation and Deep Electromagnetic Monitoring

Slob, E.C.; Draganov, D.S.; Eltayieb, M.F.M.I.; Drijkoningen, G.G.; Werthmüller, D.; Ghose, R.

DOI
10.3997/2214-4609.202120260

Publication date
2021

Document Version
Final published version

Published in
NSG2021 27th European Meeting of Environmental and Engineering Geophysics

EAGE

CONFERENCE & EXHIBITION
NEAR SURFACE GEOSCIENCE'21

Examples of seismic shallow subsurface characterisation and deep electromagnetic monitoring

E. Slob[1], D. Draganov[1], M. Eltayieb[1], G. Drijkoningen[1], D. Werthmüller[1], R. Ghose[1]

[1] Delft University of Technology

Summary

Difficulties in detecting and characterising shallow objects close the surface with seismic shear waves are often problematic because of dominant surface waves. By sequencing a specific combination of two data driven processing steps followed by diffraction tomography can overcome these problems. Small scattering objects become visible in the final image that can have importance of the understanding of subsurface locations, such as areas of archaeological interest. On the other hand, deep changes in the electric resistivity on land are often problematic to detect and especially to monitor time-lapse change over long periods of time. The usual electrodes slowly erode and vanish. Geothermal heat production environments often lead to changes in the resistivity between in-situ water-filled formations and cooler injected water-filled formations of less than one order of magnitude. A dedicated set of capacitively coupled electrode could overcome to erosion problem. When placed in a well with composite casing, these could be used in measurements of much enhanced detectability. In that case it is necessary to have electrodes in a zone from below to above the target layer. By changing the source offset at the surface, optimal measurements can be done to detect the small and deep changes in resistivity.

Small object detection and initial feasibility study for geothermal heat production monitoring

Introduction

The detection of small near surface objects and the monitoring of volumetric dynamics of injected cold water are two difficult problems for geophysical techniques to be successfully applied. We look at a shallow subsurface field example from archaeology and a deeper numerical example from geothermal production monitoring.

Detecting small objects close to but below the ground surface is challenging in most situations. First because the first few metres below the surface consist often of unconsolidated soil with variable water content, or weathered rock formations. In any case they often exhibit a high degree of heterogeneity. Second, their seismic response is usually masked by, e.g., surface waves. Thus, instead of the standard seismic processing, we use a workflow based on seismic interferometry (SI) (Place et al., 2019) and diffraction imaging (Shtivelman et al., 2009). We show a field example from archaeology to illustrate the method.

When hot water is being pumped out from the ground for geothermal heat production, it is cooled and returned to the subsurface in a different location. While the process continues the injected cooler water will flow towards the production well and heat up by the surrounding formation water and the host rock formation. Slowly the cold water volume increases and spreads out in the heterogeneous reservoir. The porosity and permeability distribution in and around the reservoir layer determines to an important degree how this cooler water volume takes shape and spreads through the reservoir on its way to the production well. Obtaining information on how this process evolves can be valuable for production management. Harmonic pulse tests are being developed and used but assume the spreading away from the injection well is cylindrical (or spherical if the layer is thick compared with the injection area). Another but different and shallow application is seasonal storage and production of heat in shallow aquifers (Fokker et al., 2021). Such changes translate themselves in electric resistivity changes, but such changes can be small. In recent years, the controlled source electromagnetic (CSEM) electric current source has increased in strength by an order of magnitude. At the same time, the noise floor of electric field receivers has been reduced by the same order (Hanssen et al., 2017). Land CSEM equipment can build on these developments and make land CSEM a viable option. Controlled source electromagnetic methods should soon deliver detailed resistivity structures, especially in joint inversion with seismic data (Panzner et al., 2016). We aim for surface sources of electric current and capacitively coupled electrodes placed in a borehole with composite casing. With such measurement setup we build the potential of being able to perform time-lapse measurements for several decades, because there is no chemical interaction between the electrodes and the surroundings. We show a numerical example to illustrate the idea.

Method and Theory

For near surface object detection, we first suppress the surface waves in a data-driven way. This is done by first predicting the surface waves using seismic interferometry, followed by removing them from the data using adaptive subtraction. After the surface waves have been subtracted, the revealed scattering events are strengthened by cross-coherence based supervirtual interferometry as explained in Place et al. (2019). Finally, we apply diffraction imaging (Shtivelman et al., 2009) with phase-weighted stacking to stack coherently over the strengthened scattering events. We apply this to data from an archaeological finding.

For monitoring, we are interested in a base case scenario and a change in the target zone after some time, or after several production and storage cycles. In our example here we limit ourselves to a feasibility study of using a surface electric current source and we assume electrodes are available in the vertical borehole with which we measure the vertical potential difference between two electrodes in the well from surface to below the target layer. Assuming that the noise reduces with increasing depth due to attenuation of magnetotelluric currents, we judge that changes due to production of hot water and injection of cool water is visible in these measurements when the measurements differ by 10% or more

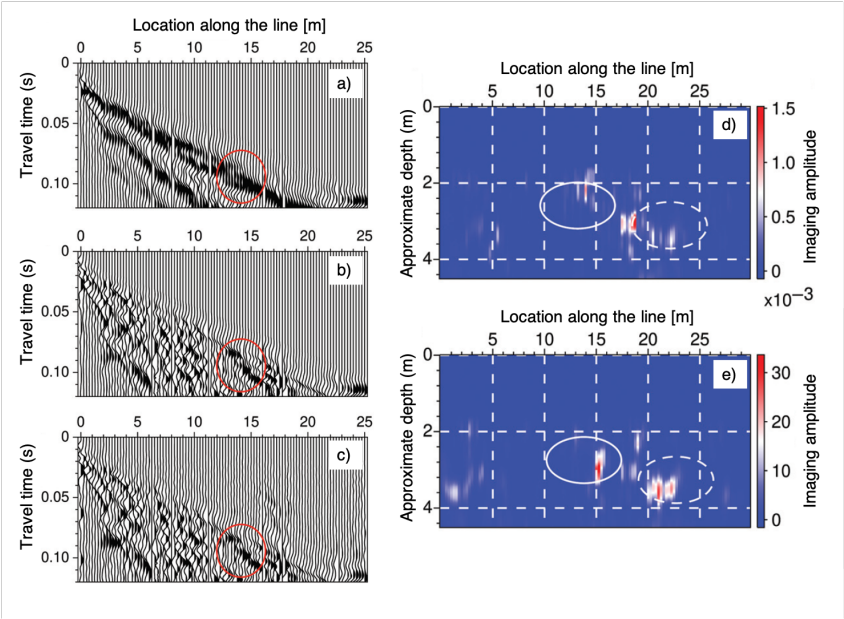

Figure 1 *a) Example SH-wave shot gather, dominated by strong Love waves, from field data acquired over a burial mound using a seismic vibrator. b) Result after Love-wave suppression by seismic interferometry and adaptive subtraction; c) The gather from b) after diffraction enhancement by supervirtual interferometry. d and e) Result from diffraction imaging using data as in b) and c), respectively. Red circles indicate scattering events, while ellipses – imaged scatterers. Modified from Liu et al. (2021).*

and the unit strength source response has an electric field of 0.1 nV/m or more. Once detectability is established it is useful to see what the largest electrode spacing can be to still observe time-lapse changes.

Field and numerical examples

A shot record of a horizontal shear (SH) wave survey is shown in Figure 1a), which is visibly dominated by surface waves and direct arrivals. After prediction and adaptive subtraction of the surface waves from the data, subsurface scattering has become visible as shown in Figure 1b). In the second step, we strengthen the revealed scattering arrivals by crosscoherence-based supervirtual interferometry followed by diffraction imaging with phase-weighted stacking to stack coherently over the strengthened scattering events and the same shot record is shown in Figure 1c). Figure 1d) shows the diffraction image obtained from the data after surface wave removal as shown in Figure 1b, while Figure 1e) shows the diffraction image obtained from the data after the new processing strategy that is shown in Figure 1c).

The model for the geothermal monitoring is a 1D approximation of the subsurface below Delft University of Technology campus where a geothermal heat production system will be built and used for campus heating. The geothermal wells will be drilled as a doublet from a single surface location and deviate at depth to a final lateral distance between injection and production locations of more than 1.5 km at production level in the reservoir, which is at just below 2 km depth. The layered resistivity model is shown in Figure 2. The black lines indicates the base case and the dashed lines the time-lapse or monitor case. The difference between the base case and the monitor case is a factor 3.3 increase in resistivity in the reservoir layer only. The reservoir is modelled as a 200 m thick layer starting at 2300 m below surface.

Modelling codes to generate data for such configurations are available as open-source software (Hunziker et al., 2015; Werthmüller, 2017), and we use empymod. Figure 3 shows the amplitude of the vertical component of the electric field generated by an x-directed electric current source operating at 0.1 Hz and located at the origin of the (x,z)-plane of the base case in the left graph where the colours indicate the amplitude and the black lines with arrows indicate the vector direction of the electric field

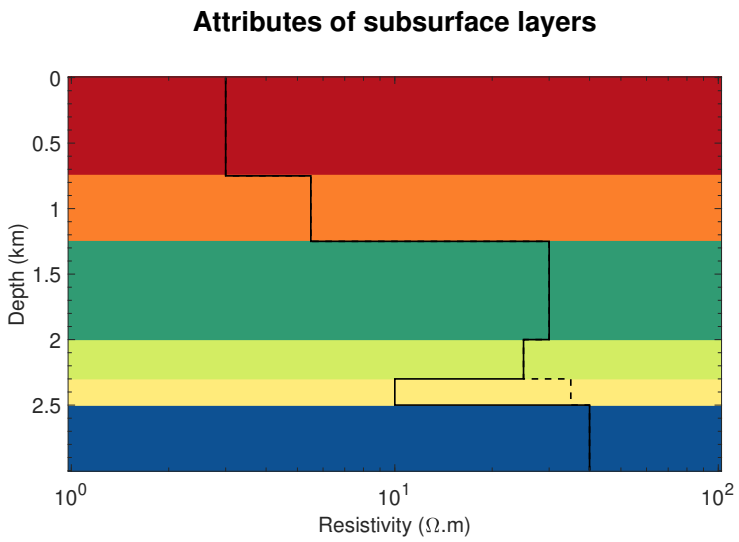

Figure 2 *Electric resistivity model as a function of depth where the colours indicate the resistivity that is shown in the black line; the values that belong to the colours can be read off from the horizontal axis. The dashed line marks the time-lapse change.*

in the subsurface. The middle graph shows a similar result but then for the monitor situation. The right graph shows the amplitude of the normalised difference in the vertical electric field where the colours indicate the strength of the relative difference in a logarithmic scale.

Results

The result of the new processing strategy for near surface object detection pays off very well. Figure 1e) is an enhanced image of subsurface objects compared with the image in Figure 1d), which can be seen especially in the amplitudes. The two objects might correspond to stones at the burial level of the burial mound over which we recorded the data.

The results for the monitoring example can be used as follows. The field vector directions in the subsurface indicate where the vertical component of the electric field is large or small and where this component is changed most due to the time-lapse changes. These are the locations where a monitor borehole should be located relative to the source location. Or, when the electrodes are placed in the injection well, at what lateral distance the electric current source should be located. The amplitude of the normalised difference in the vertical electric field shows that changes that occur in a depth range between 2300 m and 2500 m depth cannot be expected to be detected with receivers in the first 1.5 km below surface at any reasonable offset. Changes of more than 10% occur for all offsets inside the reservoir layer and to a zone that starts at 2 km depth at zero offset and reduces to just less than 1.5 km depth at 3 km offset. That gives a large range of locations or source-borehole offsets to investigate such changes over time. Below the reservoir the offset range is reduced to approximately 1.5 km. These ranges depend on the actual resistivity values in and around the target reservoir layer and should be used with care and keeping this dependency in mind. Furthermore, this numerical test is strictly 1D. Offset ranges will reduce when the time-lapse changes reduce to a cylindrical zone around the injection well and will change in general even more, and in less predictable ways, when the cold/hot water front becomes diffuse and non-circular due to heterogeneous hydraulic permeability leading to possible preferential flow paths. The latter case is the most interesting because if electromagnetic measurements could help defining the time evolution of non-symmetrical spreading, it would be helpful for production management.

Conclusions

We have shown that data-driven techniques to removing surface waves from shallow shear wave surveys can enhance subsurface scattering that come from shallow objects. We have also shown that a new

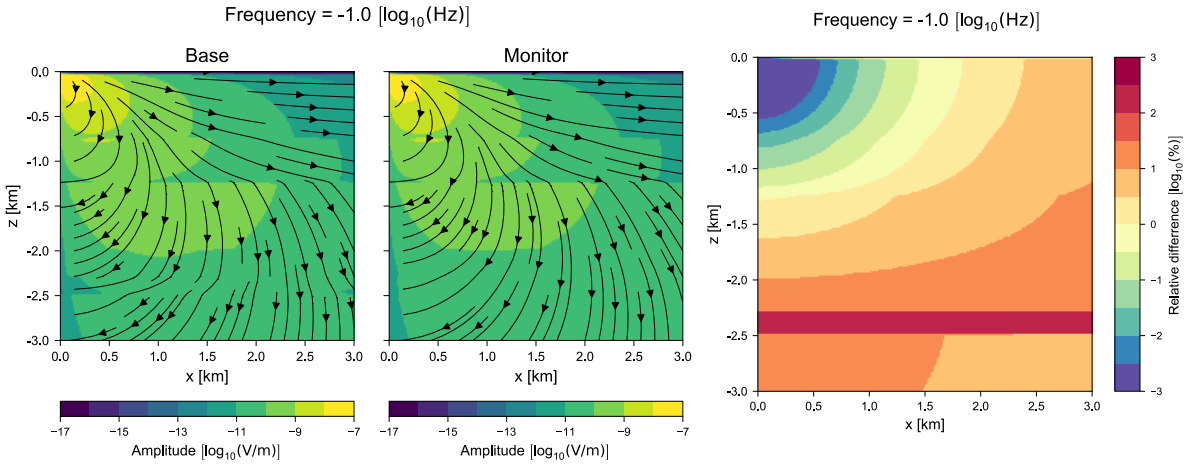

Figure 3 *The amplitude of the vertical component of the electric field is shown in colour and the electric field vector direction is shown with arrows in the (x,z)-plane for an x-directed electric current source operating at 0.1 Hz in the origin in the base case (left) and in the monitor case (middle) together with the relative amplitude of the difference in the vertical electric field component (right).*

processing and imaging workflow can improve the final image where such shallow subsurface objects can be identified with confidence.

For the monitoring example with CSEM data, we have shown that a monitoring well seems necessary to detect resistivity changes that are less than an order of magnitude in strength as we expect in a geothermal well with moderate temperatures of around 75 to 80 degrees. The injection well could be a good well to monitor changes due to injection and production. In such cases, having electrodes in a depth range from 10% above to 10% below the target depth is sufficient to detect such changes with difference of more than 10% and with field strengths that are high enough to measure these fields with sufficiently small errors. Even though the time-lapse change occurred in 1D in the example shown, such localised changes in 3D will always have a local effect when they occur in a limited and possibly irregularly shaped zone around the injection well. It seems interesting to expand the feasibility study and investigate more realistic cold water front dynamics by including flow models in the study.

References

Fokker, P.A., Borello, E.S., Viberti, D., Verga, F. and Wees, J.D.V. [2021] Pulse Testing for Monitoring the Thermal Front in Aquifer Thermal Energy Storage. *Geothermics*, **89**, 101942.

Hanssen, P., Nguyen, A.K., Fogelin, L.T.T., Jensen, H.R., Skarø, M., Mittet, R., Rosenquist, M., Súilleabháin, L.O. and van der Sman, P. [2017] The next generation offshore CSEM acquisition system. In: *SEG International Exposition and 87th Annual Meeting*. SEG, Tulsa, 1194–1198.

Hunziker, J., Thorbecke, J. and Slob, E. [2015] The electromagnetic response in a layered vertical transverse isotropic medium: A new look at an old problem. *Geophysics*, **80**(1), F1–F18.

Liu, J., Draganov, D., Ghose, R. and Bourgeois, Q. [2021] Near-surface scatters detection at archaeological sites based on interferometric workflow. *Geophysics*, **86**(3), WB1–WB11.

Panzner, M., Morten, J.P., Weibull, W.W. and Arntsen, B. [2016] Integrated seismic and electromagnetic model building applied to improve subbasalt depth imaging in the Faroe-Shetland basin. *Geophysics*, **81**(1), E57–E68.

Place, J., Draganov, D., Malehmir, A., Juhlin, C. and Wijns, C. [2019] Crosscoherence-based interferometry for the retrieval of first arrivals and subsequent tomographic imaging of differential weathering. *Geophysics*, **84**(4), Q37–Q48.

Shtivelman, V., Keydar, S. and Mikenberg, M. [2009] Imaging near-surface inhomogeneities using weighted multipath summation. *Near Surface Geophysics*, **7**, 171–177.

Werthmüller, D. [2017] An open-source full 3D electromagnetic modeler for 1D VTI media in Python: empymod. *Geophysics*, **82**(6), WB9–WB19.